THREE-DIMENSIONAL SHOCK WAVE REFLECTION TRANSITION

B.W. SKEWS[a], J.A. MOHAN

Flow Research Unit, University of the Witwatersrand, Johannesburg, PO WITS, 2050, South Africa

[a]Corresponding author: Tel.: +27117177324; Fax: +27117177049; Email: beric.skews@wits.ac.za

KEYWORDS:

Main subjects: gas dynamics, flow visualization, numerical simulation
Fluid: supersonic flow, shock wave interactions
Visualization method(s): shadowgraphy, Laser vapor screen, CFD
Other keywords: Three-dimensional processing

INTRODUCTION

It has been established that the shock wave reflection pattern on a plane surface below a supersonic body comprises of regular reflection immediately below the body, which then transits to Mach reflection in the lateral direction [1] as shown in Fig. 1a. In two-dimensional studies of wave reflection between two finite width wedges placed symmetrically in a supersonic wind tunnel it became important to examine the aspect ratio of the wedges and the consequent possible influence of a finite width wedge causing the intrusion of three-dimensional flows [2]. This flow field is presented schematically in Fig. 1b and also shows the transition in the transverse direction. Whilst the transition conditions between regular and Mach reflection in the two-dimensional case have been well researched and described (see the treatment by Ben-Dor [3]), there has been limited assessment of the three-dimensional case [4]. This latter work only examined where the transition occurred on the reflection plane but did not examine its nature.

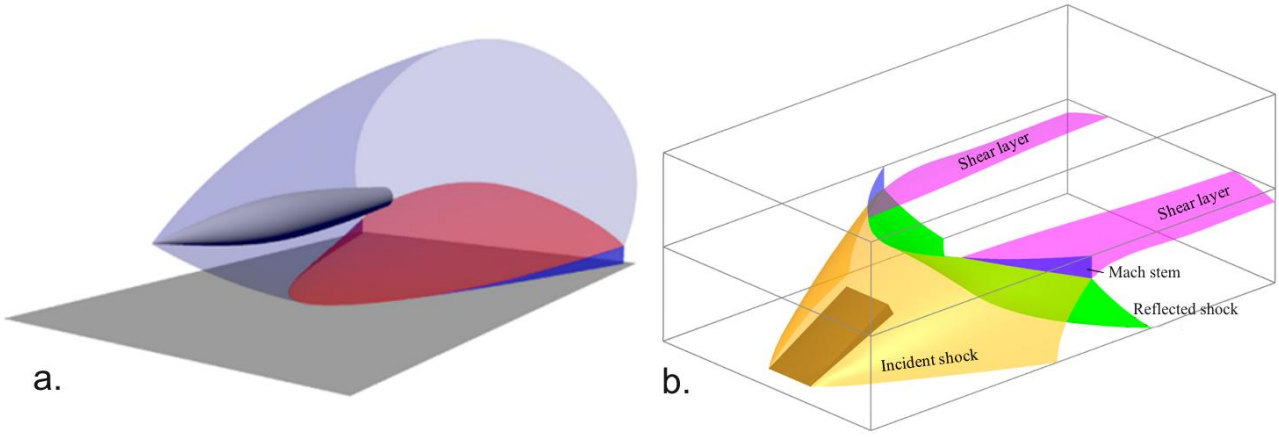

Fig. 1. a) Wave pattern around a supersonic body interacting with a ground plane
b) Lower half wave pattern between two wedges showing reflection off the symmetry plane.

THE DOUBLE-WEDGE ARRANGEMENT

The test model used in the supersonic wind tunnel is shown on the left in Fig. 2. It is arranged that the two wedges move together by rotation of a calibrated knob so as to maintain a symmetry plane midway between them. Wedges with aspect ratios of 0.5 and 1.0 were used in order to generate the three-dimensional flow with the reflection transition points within the field of view. Tests were run at a nominal Mach number of 3.1. Because of the flow of interest being three-dimensional it is necessary to view the flow from different directions. This is achieved by having the whole optical system mounted on a frame suspended from the ceiling which has motion in roll, pitch and yaw about a centre in the wind tunnel centreline. This is also shown in Fig. 2. A contact shadowgraph optical system is employed.

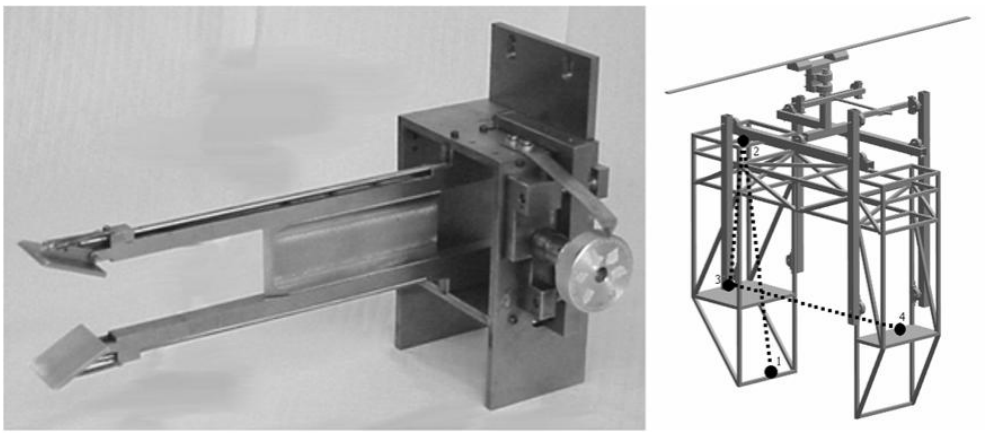

Fig. 2. The adjustable double-wedge test piece and the support frame for the optics. Components are as follows: 1- light source, 2- parabolic mirror, 3- plane mirror, 4- photographic film (no lens). Dotted line shows the optical path.

Conventional results taken with the optical axis normal to the wind tunnel windows are given in Fig. 3, for two different wedge incidence angles. In the first case with a wedge incidence of 20 degrees regular reflection between the upper and lower incident shocks persists throughout the field of view. There is a slight indication of two slightly displaced lines downstream which are the lines of regular reflection on the two sides of the vertical symmetry plane and are visible due to some slight misalignment between the model orientation and the optical axis. The second case is with the wedge angle increased to 28 degrees. There is a clear feature behind the front reflection point which is on the vertical symmetry plane. This feature images the growing peripheral Mach stem surface on both sides of this symmetry plane.

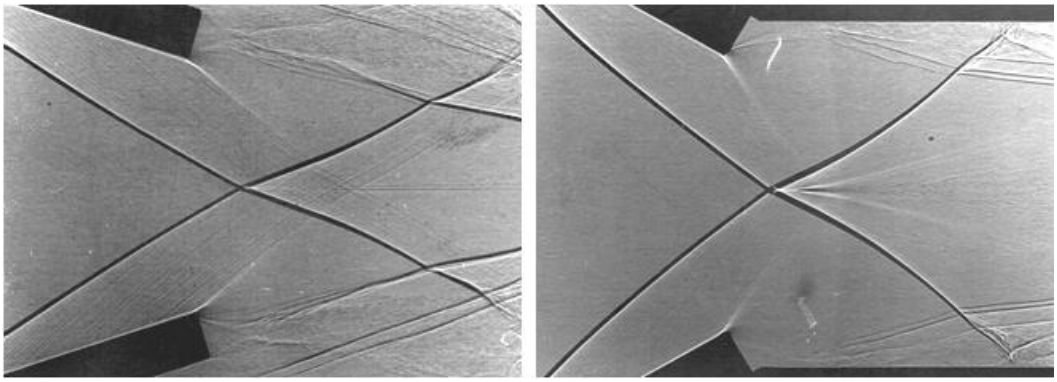

Fig. 3. Shadow images of regular reflection on the vertical symmetry plane with wedge angles of 20 and 28 degrees.

If the optical axis is yawed and/or rolled in order to be able to see the transition points on both sides of the flow field images such as those in Fig 4 are obtained.

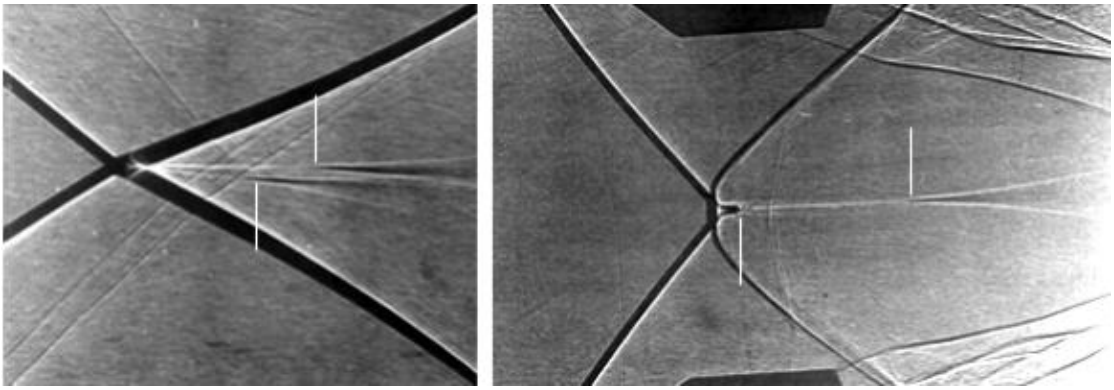

Fig. 4. Oblique imaging. Left: slight yaw and roll. Right; 45^{o} yaw. Vertical lines show the transition point

The abrupt change in Mach stem height is somewhat surprising and besides repeated efforts could not be reproduced through simulation. This transition geometry clearly requires further investigation. In addition, there is also an indication of instability in the transition point as shown in the enlargement in Fig. 5a. Further complications arise because of the shear layer obscuring the point of interest with zero yaw, as shown in Fig. 5b, and significant difficulties with interpretation with further optical angle adjustments as in Fig. 5c. An alternative method is thus sought to generate the required three-dimensional transition as discussed below.

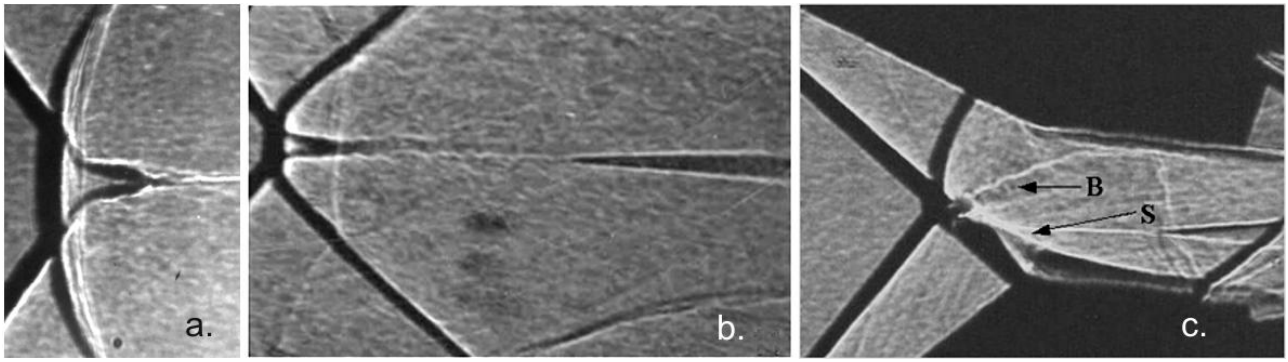

Fig. 5. Problems of interpretation using this technique: a) transition instability, b) obstruction by the shear layer, c) interpretation difficulties.

THE WEDGE-CONE ARRANGEMENT

It has been well proven that the reflection on the axis of symmetry of a conical wave will always be Mach reflection. On the other hand, as shown above, the reflection between two symmetrical wedges will be regular reflection for small wall angles. Combining these boundary conditions leads to an inferred combination between them as shown in Fig. 6. Thus there will be a transition from Mach to regular reflection in a way to be determined. The result will be a merging of the one reflection pattern with the other with the associated complex interaction between the associated wave systems.

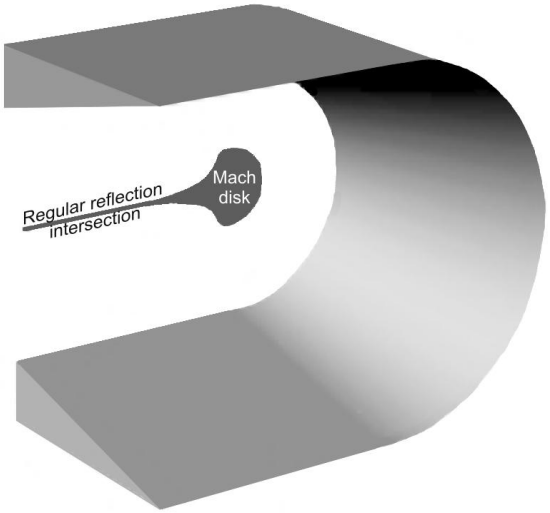

Fig. 6 The wedge-cone geometry

Since in some cases direct visualisation is impractical because of the blockage caused by the conical cap, the laser vapour screen technique, LVS, was employed. The photograph has to be taken at an angle to the laser sheet since the camera is outside the tunnel and this results in a foreshortening of the images. Where the pattern of interest occurs downstream of the model conventional shadowgraphy is used.

The tests were conducted in a blow down type wind tunnel. The cross-section of the tunnel test section is 100x100 mm with the tests being run at a nominal Mach number of 3.2.

Numerical simulations were conducted using the commercially available code, Fluent 6.2.16. The calculations were performed as inviscid. All wall boundaries were modelled as free slip walls. Post-processing involved the production of slices of the flow at relevant points on the model. The two-dimensional CFD images were imported into the NURBS (Non Uniform Rational B-Splines) surface modelling software package, Rhinoceros , to generate three-dimensional models. The salient features are traced for each of the components of the flow and the traces converted to a surface for each of them.

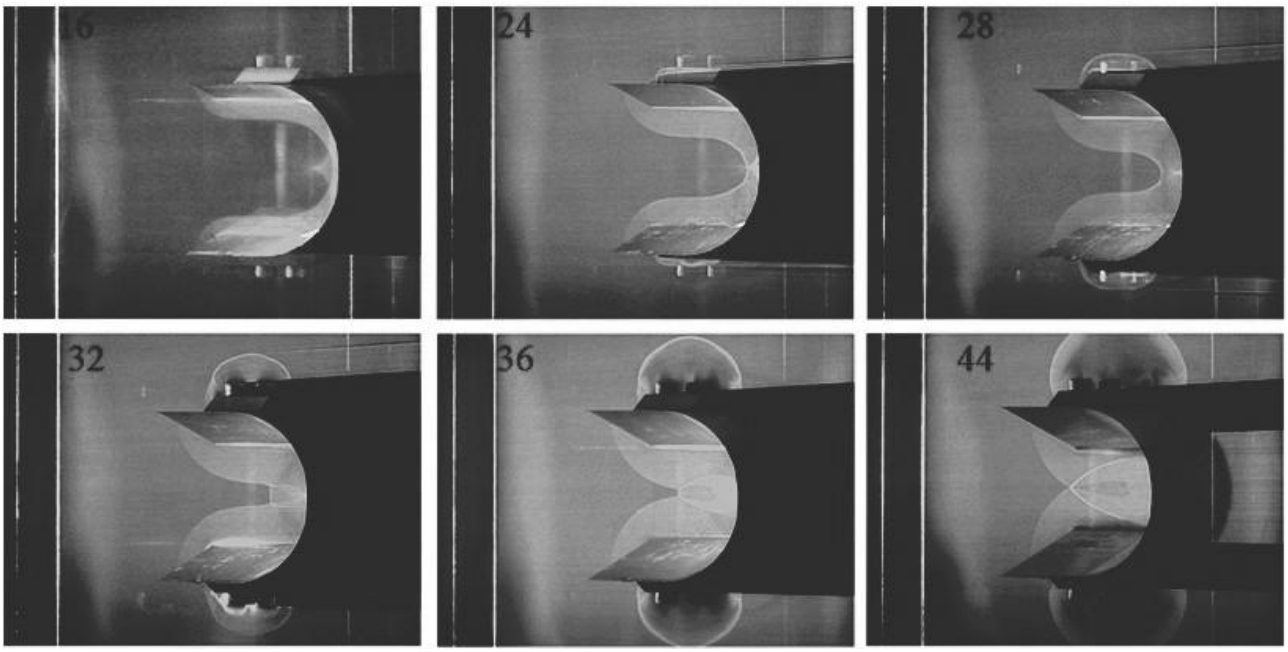

Fig. 7. Typical LVS results. 15° wedge angle, 20 mm wedge span, 39 mm chord, 10 mm trailing edge radius. Distances, (in mm) are measured from the leading edge.

A typical set of results of the flow cross-sections, successively moving the laser sheet towards the trailing edge, and beyond, is given in Fig, 7. At 16 mm the plane reflected wave off the wedge is connected at one end to its diffracted shape around the edge of the wedge, and at the other to the circular section of the conical shock. Further into the flow kinks develop on this curved section and then break down into two triple points with a Mach stem between them. Reflected waves and shear layers then arise from these triple points. The Mach stem reduces in size further back. The incident waves then reflect off each other on the plane of symmetry in a regular fashion, and enclose the previously shed shear layer.

A comparison between CFD simulation and LVS imaging for a 10° wedge angle with a larger span of 30 mm is given in Fig. 8. There is a close match between them so the simulation can be used with confidence in the generation of three-dimensional surface models. A new bridging shock appears between the reflected wave from the Mach reflection and those from the regular reflection.

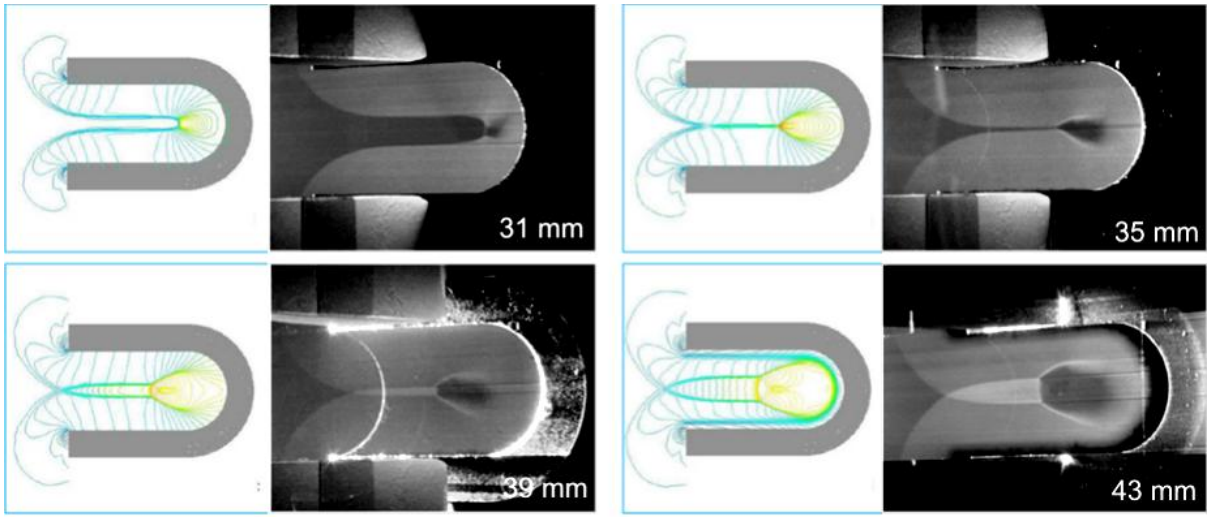

Fig. 8. Comparison between CFD and LVS results. 10° wedge angle, 30 mm wedge span, 39 mm chord, 10 mm trailing edge radius. Distances are measured from the leading edge.

Patterns of the flow in planes on or near the longitudinal symmetry plane are given in Fig. 9. These show the rather complex patterns that are difficult to interpret using two-dimensional cross sections. However, the high density region behind the Mach stem and bridging shock become clear as also indicated in the plots of Fig. 8.

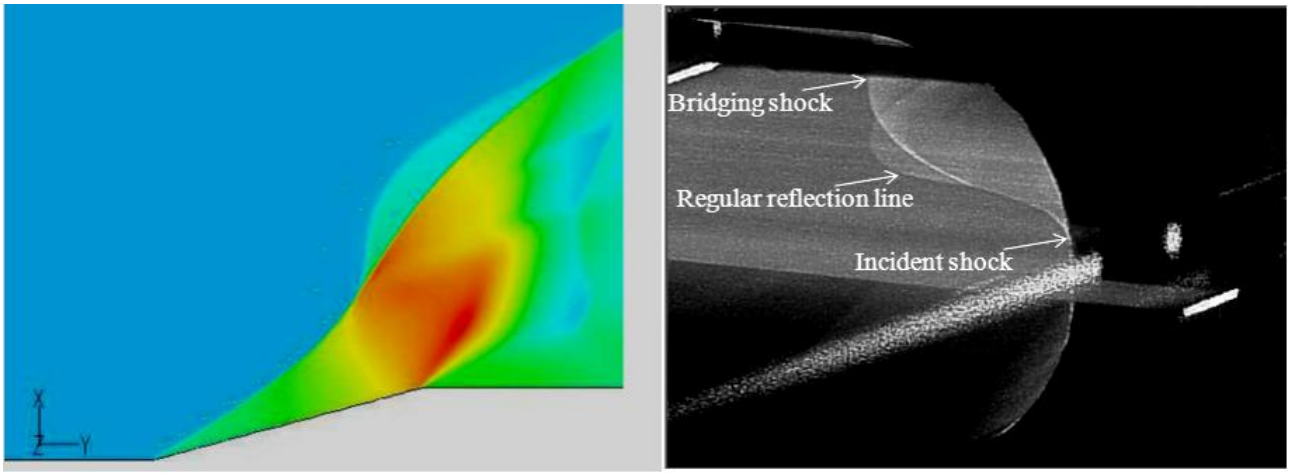

Fig. 9. CFD density flood plot in the longitudinal symmetry plane and LVS image from 2 mm below this plane. 15° wedge angle, 20 mm wedge span, 39 mm chord, 10 mm trailing edge radius.

In the case of a 10° wedge and shorter chord the interactions of interest occur downstream of the trailing edge of the model and therefore are amenable to conventional visualization techniques. In order to avoid the effects of the end diffraction a conical cap is added to that end. Fig. 10 is a shadow image showing the flow through the major axis plane, together with streamline patterns in the major axis and minor axis planes, coloured by Mach number. It is interesting that the line of intersection of the plane shocks arising from the wedge leading edge, before being influenced by the curved shocks from the conical surfaces does not show up on the shadowgraph. This is because immediately on either side of the line of reflection light rays do not get deflected. Strong shear layers emanate from the meeting of the edge of the Mach surface and this regular reflection line. The position of the Mach stem is clear in the major axis streamline pattern as is indicated by the low velocity green contours. The bridging shock is clearly visible in Fig. 10c.

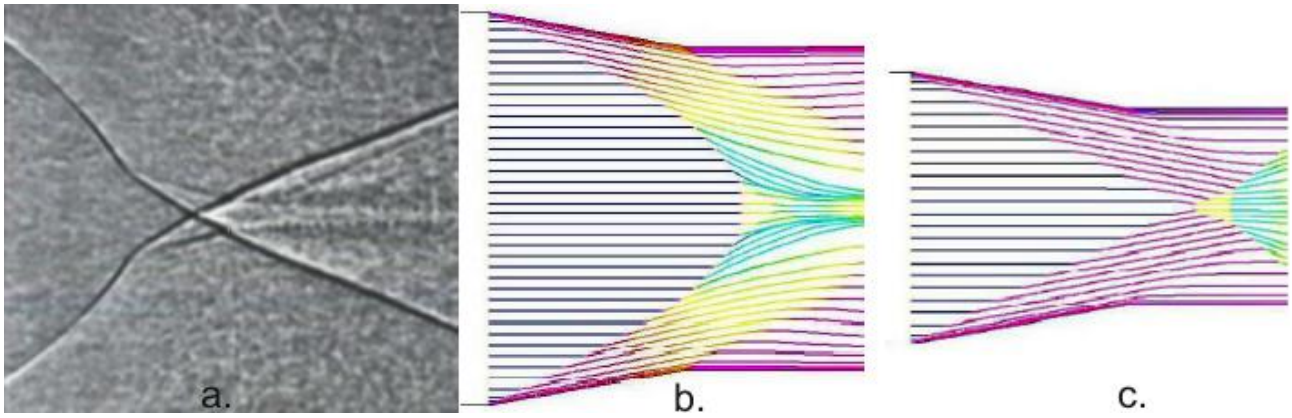

Fig. 10. a) Shadowgraph through the longitudinal symmetry plane. b&c) Streamline patterns coloured by Mach number in the major and minor axis symmetry planes. 10° wedge angle, 20 mm wedge span, 27.5 mm chord, 11.7 mm trailing edge radius

Because of the complexity of the shock wave interactions and the associated flow fields it is useful to generate three-dimensional surface models which may then be rotated and viewed from any direction as well as being presented as animations. Two examples are presented below in order to show the relationship between the various features.

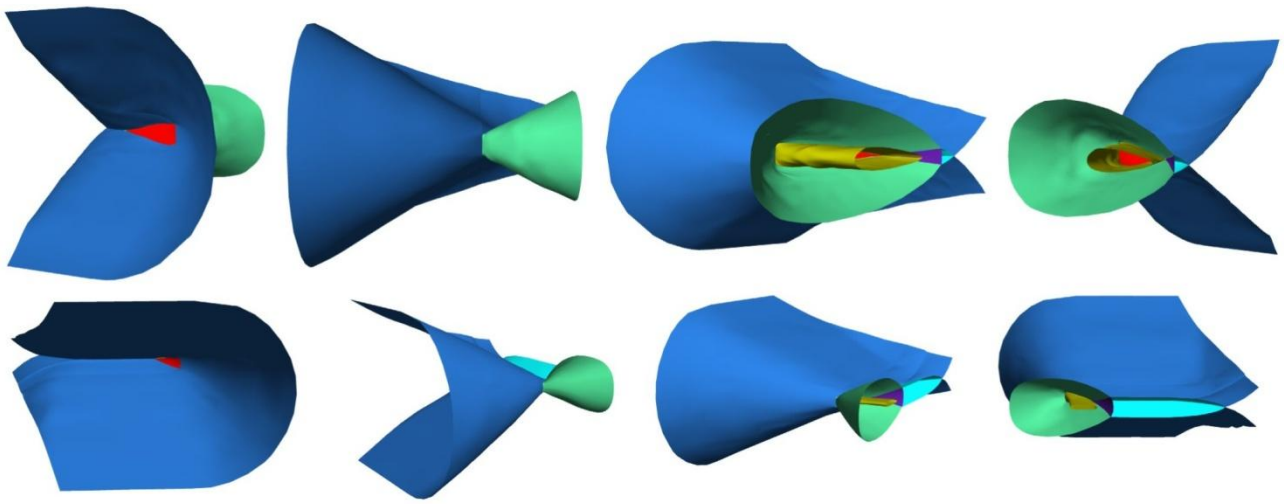

Fig. 11. Surface models for the 15° wedge with 20 mm span (top) and the 10° wedge with 30 mm span (bottom).Blue - incident shock, Red - Mach disk, Green - reflected shock from Mach reflection, Cyan - reflected shock from regular reflection, Purple - bridging shock, Tan - shear layer

One of the benefits of this surface modeling is that individual components may be removed or made semi-transparent so as to understand the connections and interrelationships between the components as shown in Fig. 12. This clearly shows the common meeting point, in space, between the Mach disk, shear layer, reflected waves from the regular reflection, and the bridging shock. It is at this point that the transition from Mach to regular reflection occurs.

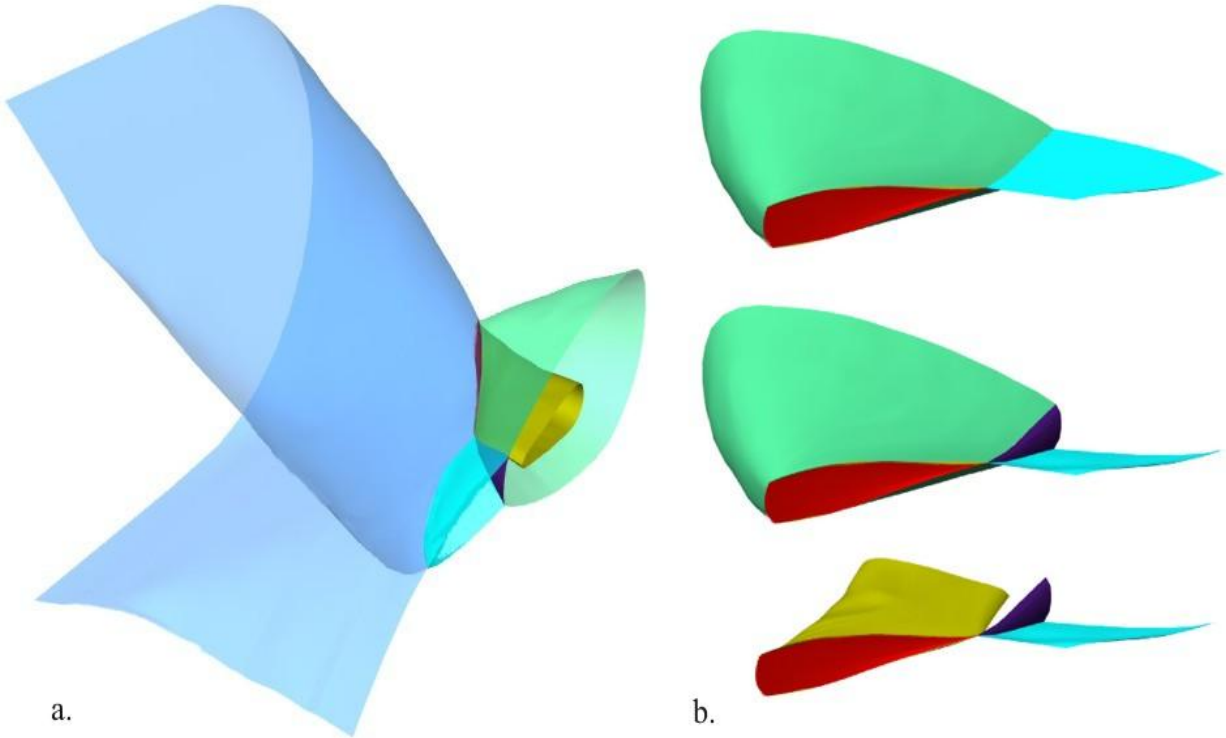

Fig. 12 Surface manipulations. a) the effect of transparency b) successive removal of features starting with the incident shock, then upper reflected shock from the regular reflection, and then the reflected shock from the Mach reflection. This leaves the Mach disk, lower reflected shock from the regular reflection, the bridging shock and the shear layer.

CONCLUSION

Cases of the three-dimensional transition between regular and Mach reflection are identified. An alternate approach is adopted to generate these transitions by combining the flow between two wedges with that from a half conical surface. A flow field results which demonstrates the complexity of the interaction in that at the transition point besides the incident and reflected waves from both the regular and Mach reflection, a third bridging shock develops, thereby modifying the flow still further from that between two bodies symmetrically placed in a supersonic stream with the plane of symmetry acting as the reflection plane. This work does not contribute to establishing the conditions under which the transition occurs.

Acknowledgement: This research was supported by funding from the National Research Foundation.

References

1. Marconi, F. *Shock reflection transition in three-dimensional steady flow about interfering bodies.* AIAA J. 1983, 1, 707-713
2. Skews, B.W. *Three-dimensional effects in wind tunnel studies of shock wave reflection*. J. Fluid Mech. 2000, **407,** 85-104
3. Ben-Dor G. Shock wave reflection phenomena. Springer, 2007
4. Irving Brown YA, Skews BW. *Three-dimensional effects on regular reflection in steady supersonic flows*. Shock Waves , 2004, 13, 339-349